Effect of physical variables in dynamic recrystallization during friction stir welding of aluminum alloy

[1]Haftu Hagazi Hadgu
[1]Lecturer
[1]Department of Mechanical Engineering
[1]College of Engineering and Technology, [1]Adigrat University, Adigrat, Ethiopia

***Abstract*— Tailoring microstructure in single pass or multipass deformation process is one of the cutting edge research areas in several applications of engineering problems. An accurate knowledge of the overall temperature distribution, strain and strain rate are prerequisites for reliable prediction of final microstructure and mechanical properties of the deformed products. One typical application of heavily deformed process is observed in friction stir welding (FSW) which is one of the emerging solid state joining processes where the material is processed by extreme plastic deformation associated with the frictional straining. FSW is subjected to variable temperature, strain and strain rate at different zones of welded sample. The domain of interest passes through variable range of physical parameters i.e. temperature, strain and strain rate. Also, the variability exists due to different process parameters like tool rotational speed, welding speed and additional external heat source of hybrid FSW process. The recrystallization kinetics is not well understood for FSW process. For aluminum alloy, the material undergoes various thermal and mechanical histories that strongly influence the final microstructures through prevailing of preferably continuous dynamic recrystallization over a wide range of temperature and strain rate. The recrystallization mechanism plays a significant role on grain refinement and finally influences the weld joint strength. This process determines the microstructure and properties of welded joint and it is imperative to gain better understanding and control of recrystallization process in this circumstances. In the present work, an investigation is carried out on recrystallization mechanism as a function of temperature, strain and strain rate during FSW process. An analytical model for continuous dynamic recrystallization has been developed to predict average size of friction stir welded sample for different process variables.**

***Index Terms*— Dynamic recrystallization, grain refinement, severe plastic deformation, aluminum alloy, friction stir welding**

I. INTRODUCTION

There is continuous growing interest in production of ultrafine and nanocrystalline microstructures by severe plastic deformation. It emphasized on fundamental understanding of recrystallization mechanism in large strain deformation. Friction stir welding (FSW) or processing is fundamentally a hot-working process involves large plastic deformation in which the process variables are represented as rapid transients and steep gradients in strain, strain rate, and temperature [1]. Most of the analysis of severe plastic deformation process is simplified by uniform strain and isothermal conditions because of the difficulty in experimentation. Although, FSW process finally determine the microstructure and properties of welded materials, it is imperative to gain better understanding and control of recrystallization in presence of rapid transients and steep gradients of process variables.

In FSW, due to complex strain path and alloys, empirical relation follows the interpretation of dynamic recrystallization. However, FSW technology involves severe plastic deformation (SPD) under the condition of steep gradient of temperature, strain, and strain rate. The weld nugget zone experienced with large plastic strain at strain rates of ~ 10 - 100 1/s and peak temperature of ~ 0.6 to 0.95 times of melting point [1]. The microstructures are typically highly refined as compared to base material. The thermo-mechanically affected zone (TMAZ) experiences lesser strain, strain rates as well as low peak temperature and is characterized by grain distortion that may lead to refined, and equiaxed grains at the interface of nugget and TMAZ. The heat affected zone experiences only thermal cycle. During FSW, the original grain and sub grain boundaries appear to be replacing with fine, equiaxed-recrystallized grains in the weld nugget. It is unlikely that dynamic recrystallization occurred via a 'discontinuous' process. Rather, it appears that a 'continuous' dynamic recrystallization (CDRX) process, analogous to that which gives rise to sub grain formation during hot rolling. The conventional hot working process like rolling, forging and extrusion also reaches the strain rate of 1 – 100 s^{-1} at temperature more than 0.5 times of melting point temperature. The difference in FSW process is in terms of transients and gradients in strain. Combinations of grain size strengthening with strain hardening and other strengthening mechanisms may enable production of fully efficient joints in FSW of materials that are not acquiescent with conventional heat treatment process.

Jata et al. [2] have investigated the microstructural changes during FSW of Al-Li-Cu alloy of 7.6 mm thick plate. The parent material contains elongated grains of ~ 150 μm long and ~ 75 μm thick along with subgrains of 2 – 10 μm. Large amount of misorientation exists at 10˚ as well as 60˚. After deformation by FSW process, the microstructure consists of average grain size of ~ 9 μm and misorientation distribute almost equally between 10˚ to 60˚.

To modify the microstructure of friction stir welded sample, post-weld heat treatment often create abnormal grain growth (AGG) of aluminium alloys (7474, 7050, 7075, 2024, 2519, etc.) and non-heat-treatable aluminium alloys, like 5083. However,

commercially pure aluminium does not show this behaviour [3 - 5]. The primary factors leading to AGG in stirred materials are associated with the inhomogeneous deformation pattern during welding. Certain combinations of tool rotation rate and traverse rate eliminate AGG suggests that microstructural uniformity is one key aspect for avoiding AGG. However, thermal input and material flow must be considered together to develop a comprehensive understanding of AGG phenomena in friction stirred microstructures. The tool design provides another intriguing opportunity to expand the process window without AGG.

The objective of the present research was to develop a basic understanding of the nature of recrystallization and to relate it with the deformation process variables such as strain, strain rate, and temperature. However, the process variables such as strain rate in FSW are qualitatively estimated by analytical/semi-analytical method. The heat is generated by friction as well as plastic deformation which alters the microstructure and properties. The kinetics depends mainly on the temperature and strain rate and microstructure evolution influence the energy transfer within the system. The center of stirred zone (SZ) experiences dynamic recrystallization and is followed by recovered microstructure around the stirred zones at low level of deformation and temperature. A part of the plastic deformation energy is also stored within the thermomechanically affected zone (TMAZ) in the form of increased dislocation densities within the deformed grains. The heat affected zone (HAZ) is affected only by the temperature and the microstructural changes with respect to base material are insignificant.

II. THEORETICAL BACKGROUND

Several researchers have explained the mechanism of grain refinement of FSW by dynamic recovery (DRV) and recrystallization mechanism of aluminum and aluminum alloy in terms of geometric dynamic recrystallization (GDRX), continuous dynamic recrystallization (CDRX), discontinuous dynamic recrystallization (DDRX) and recrystallization at the shear bands [6 - 7]. The mechanism of DRV, GDRX and CDRX are consistent with aluminum because of its high stacking fault energy. However, the recrystallization mechanism is also influenced by the alloying elements since it can modify the stacking fault energy. Also, the variation of thermo mechanical conditions and initial grain size for the same material may change the recrystallization mode [4-5].

In DRV, the flow stress remains constant with strain because a dynamic equilibrium exists between dislocation multiplication and recovery due to dislocation rearrangement. The steady state situation is represented by constant equiaxed subgrain with nearly dislocation-free interiors, and nearly uniform subgrain boundary misorientation. The GDRX may occur when the prior boundaries are serrated by local response to the interface tension of subgrain boundaries. It develops waviness of the order of subgrain size and the prior boundary separation becomes almost equal to the subgrain size. The recrystallized grains are surrounded by a mixture of prior boundary segments and subgrain boundaries. However, GDRX does not involve long-range migration of high angle boundaries. The serrations become pinched off and equiaxed grains with HAGB are formed.

Majority of the investigation predicts that the mechanism for FSW of pure aluminium is CDRX [8 - 10]. Several mechanisms of CDRX by which subgrains rotate and achieve a high misorientation are proposed [9 - 10]. Boundary sliding with grain rotation is a feature that is characteristic of super plasticity and is not operative for high strain rate FSW process. Sub grain growth does not occur in FSW process because many of the recrystallized grains formed in the DRX region are finer than the starting sub grain size. Hence, dislocation glide-assisted-sub grain-rotation model is the most suitable mechanism for FSW process where dislocation glide gives rise to a gradual relative rotation of adjacent sub grains. The recovery and/or recrystallization in FSW may not be always complete or continuous in nature. Hence, the grains resemble cells rather than fully recovered grains. Majority of the grains may have clean boundaries with no dislocation tangles at the boundaries. A helical dislocation loop often observed in grain, which are believed to be generated during thermal quenching. Therefore, it is often required the aging treatment of aluminum alloy to have stable dynamically recrystallized zone [2]. During FSW of Al-Li alloy, the dislocation density in the subgrain boundaries increases with rolling passes, but the sub grain size remains fine due to the pinning action of the precipitates. The cell/sub grain interior is lacking dislocations, and therefore a strain gradient exists across the cell/sub grain. To maintain plastic compatibility across boundaries, the subgrains rotate to larger angles. Thus, the magnitude of the misorientation increased noticeably during FSW relative to those in the parent metal. Thus, the 'grains' observed in the weld nugget are actually high-mis orientation sub grains [2].

The theoretical basis of recrystallization mechanism in friction stir welding has explained in several ways that are proved with solid experimental investigation. However, in the present work, a working model of recrystallization is proposed with simplified calculation but considering the effect of driving parameters. The model results are validated with measured grain size of post-weld sample without any intermediate experimental investigation.

III. MATHEMATICAL MODEL

In FSW, the flow stress is highly dependent on temperature and the stain rate. Thus, the resulting grain structure mainly depends on the strain rate and temperature distributions. The strain rate is calculated from the velocity field of the material. There are two interfaces between the tool and the workpiece: one is at the shoulder and the other is at the pin (**Fig. 1)**. Two state variables are defined in radial and thickness direction respectively to consider the contact conditions between tool and workpiece material. The first one (α) relates the material velocity to shoulder velocity and is defined as a function of z. Similarly, the second state variable (β) relates the material velocity to pin velocity, which is defined at a radial distance 'r'. The state variables are expressed as [11]

$$\alpha = A \exp\left\{-B\frac{z}{z_0}\right\};\quad \beta = C \exp\left\{-D\frac{(r-R_p)}{(R_s-R_p)}\right\} \qquad (1)$$

where the constants A, B, C, D are evaluated from friction condition (between 0 and 1) including the effect of material properties, axial pressure, and temperature [11-12]. **Figure 1(b)** depicts the schematic view of linear velocity components in (r, θ) coordinates corresponding to flat tool shoulder and workpiece interface. V_T represents transverse tool speed. The velocity components on the material volume just below the tool shoulder is

$$U_{s\Theta} = \alpha[\omega r - V_T \sin\Theta];\ U_{sr} = \alpha[-V_T \cos\Theta] \quad (2)$$

The velocity at tool pin periphery has been defined as

$$U_{p\Theta} = \beta\left[\omega R_p - V_T \sin\Theta\right];\ U_{pr} = \beta[-V_T \cos\Theta] \quad (3)$$

There will the interference of the velocity field by the tool shoulder and tool pin. To account the same, the weight functions for the shoulder and the pin are defined as

$$\delta_{s\Theta} = \frac{U_{s\Theta}}{U_{s\Theta}+U_{p\Theta}};\quad \delta_{p\Theta} = \frac{U_{p\Theta}}{U_{s\Theta}+U_{p\Theta}};\quad \delta_{sr} = \frac{U_{sr}}{U_{sr}+U_{pr}};\quad \delta_{pr} = \frac{U_{pr}}{U_{sr}+U_{pr}} \quad (4)$$

Thus, the overall velocity field yields in the (r-Θ-z) coordinates as

$$U_\Theta = \delta_{s\Theta}U_{s\Theta} + \delta_{p\Theta}U_{p\Theta};\ U_r = \delta_{sr}U_{sr} + \delta_{pr}U_{pr};\ U_z = 0 \quad (5)$$

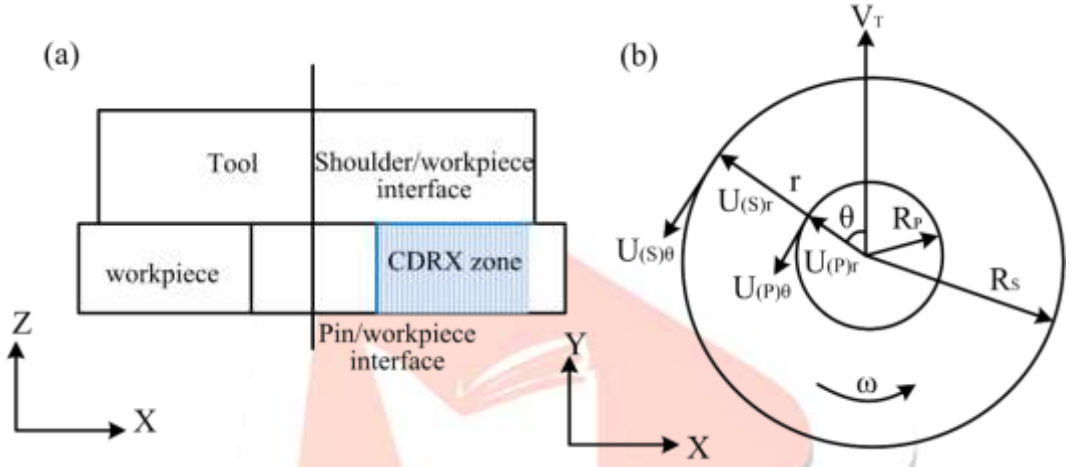

Figure 1: (a) Schematic illustration of shoulder and pin interface and (b) velocity components at shoulder/workpiece interface.

The strain-rate components are expressed as

$$\dot{\varepsilon}_{rr} = \frac{\partial U_r}{\partial r};\quad \dot{\varepsilon}_{\theta\theta} = \frac{1}{r}\frac{\partial U_\theta}{\partial \theta} - \frac{\partial U_r}{\partial r};\quad \dot{\varepsilon}_{zz} = \frac{\partial U_z}{\partial z} \quad (6)$$

$$\dot{\varepsilon}_{r\theta} = \frac{1}{2}\left[\frac{1}{r}\frac{\partial U_\theta}{\partial \theta} + \frac{\partial U_\theta}{\partial r} - \frac{U_\theta}{r}\right];\quad \dot{\varepsilon}_{\theta z} = \frac{1}{2}\left[\frac{\partial U_\theta}{\partial z} + \frac{1}{r}\frac{\partial U_z}{\partial \theta}\right];\quad \dot{\varepsilon}_{zr} = \frac{1}{2}\left[\frac{\partial U_z}{\partial r} + \frac{\partial U_r}{\partial z}\right] \quad (7)$$

The effective strain-rate ($\dot{\varepsilon}_{eff}$) assuming von Mises criteria is expressed as [12-13]

$$\dot{\varepsilon}_{eff} = \left[\frac{2}{3}\left\{\dot{\varepsilon}_{rr}{}^2 + \dot{\varepsilon}_{\Theta\Theta}{}^2 + \dot{\varepsilon}_{zz}{}^2 + \dot{\varepsilon}_{r\Theta}{}^2 + \dot{\varepsilon}_{\Theta z}{}^2 + \dot{\varepsilon}_{zr}{}^2\right\}\right]^{\frac{1}{2}} \quad (8)$$

The effective strain is also estimated as

$$\varepsilon_{eff} = \frac{\dot{\varepsilon}_{eff}}{N} \quad (9)$$

where N is the rotational speed of the tool.

Knowledge of strain and strain rate is important for understanding the subsequent evolution of grain structure, and serves as a basis for verification of various models as well. In the present work, it is assumed that the significant microstructural evolution takes place during FSW due to continuous dynamic recrystallization (CDRX) phenomena, resulted in a highly refined grain structure in the weld nugget. The analytical models aimed to the determination of the average grain size due to continuous dynamic recrystallization phenomena in FSW processes. It is obvious from literature that the recrystallization behaviour depends on initial grain size (D_i), strain (ε), strain rate ($\dot{\varepsilon}$) and temperature (T). Therefore, the CDRX model takes into account with few material constants to predict average grain size in the weld zone [14]. The empirical model is described by

$$D_{CDRX} = C_1 \varepsilon^k \dot{\varepsilon}^j D_i^h \exp\left(-\frac{Q}{RT}\right) \quad (10)$$

where (C_1, k, j, h) are constants, Q is the activation energy and R is the characteristic gas constant. The initial grain sizes are measured through experiments before welding. The distributed values of strain-rate and strain are predicted from the analytical models at different discrete points of welded sample. The temperature distribution is also estimated from a finite element based numerical model. Therefore, it is possible to develop a multi-scale model for the prediction of the distribution of average grain size in friction stir welded sample.

IV. RESULTS AND DISCUSSION

The mathematical model described in eq. (8) is used to predict strain rate and average grain size in the weld zone. The stirring action during FSW is not modelled physically in the present work. The velocity components are evaluated in discrete points. The numerical differentiation of velocity at a fixed point indicates the strain rate. The analytical estimation of strain rate is validated with the experimental results for AA 7075 material with 3 mm thick [15]. The straight cylindrical FSW tool is used with pin diameter of 3.0 mm, shoulder diameter of 10.0 mm and 2.8 mm pin height. The calculated result shows good argument with literature data (**Fig. 2)**. However, the correct estimation depends on optimum values of constants A, B, C and D. It was found that non-symmetrical strain rate distribution under tool shoulder is ~ 4.5 s^{-1} around the tool axis. The calculated strain rate is 4.8 s^{-1} which is the nearest value of experimental data.

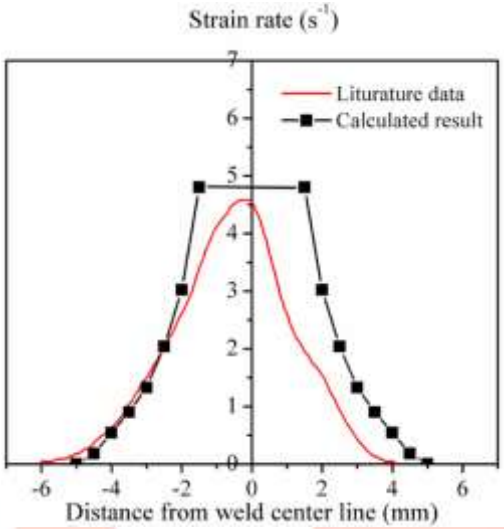

Figure 2: Validation of calculated strain rate with experimental data [15].

Table 1: Process parameters for welding of AA1100.

Exp. no.	Process parameter	
	Transverse speed (mm/min)	Rotational speed (rpm)
1	63	600
2	98	600
3	63	815
4	98	815

The strain rate depends on distance travelled by the tool in unit time and contact state condition between the tool and the workpiece. **Figure 3** shows the computed strain rate across the weld cross-section at 1 mm under the tool shoulder for different welding condition shown in **Table 1**. It shows that maximum strain rate occurs near the surface of the pin where the maximum velocity gradient exists. The strain rate rapidly decreases away from the tool axis due to rapid reduction in velocity gradient below the shoulder periphery. Beyond the periphery, the velocity gradient decreases sharply because of the rapid decay of velocity. The maximum value of strain rate achieved was 6.8 s^{-1} at welding condition of 815 rpm and 98 mm/min welding speed. It is also observed that strain rate in the recrystallized zone decreases with decrease in rotational speed.

Figure 4 illustrates the temperature distribution in the FSW joint along the transverse section at 1 mm under the tool shoulder for different welding conditions corresponding to **Table 1**. The temperature is computed from a finite element based numerical model. The temperature histories are symmetric about the weld centreline under the shoulder. The maximum temperature under the shoulder can reach up to ~ 840 K. The maximum temperature occurs at the centre of the tool that is due to the large amount of plastic deformation taking place at this region.

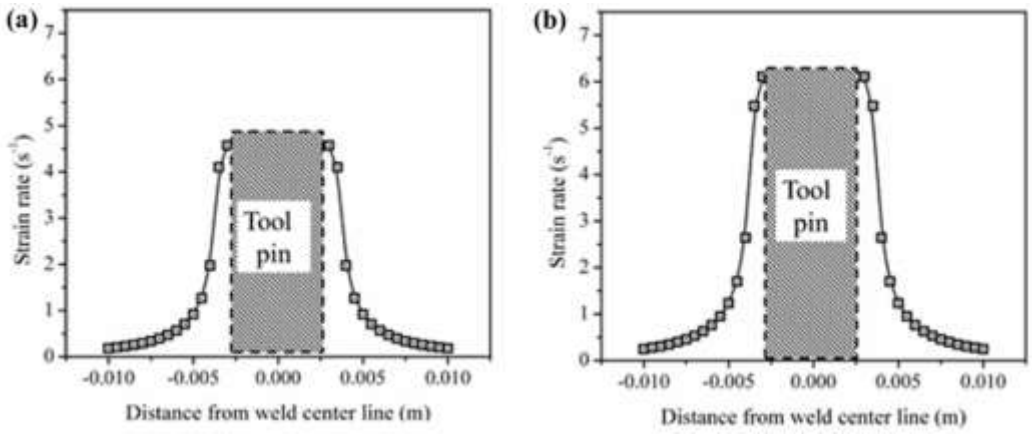

Figure 3: Strain rate at weld cross section of 1 mm below from top surface at welding condition of (a) 600 rpm and 63 mm/min, and (b) 815 rpm and 63 mm/min.

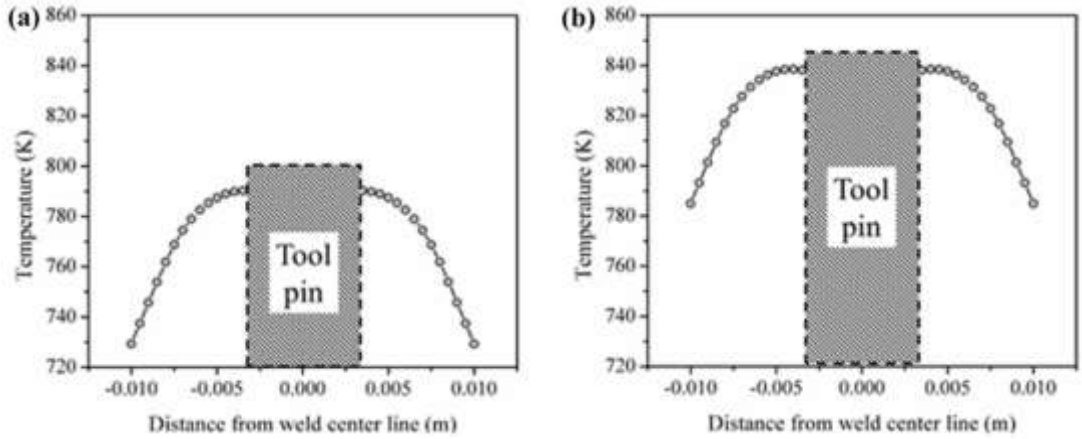

Figure 4: Temperature at weld cross-section of 1 mm below from top surface at welding condition of (a) 600 rpm and 63 mm/min, (b) 815 rpm and 63 mm/min.

The initial average grain size (D_i) is approximately ~ 98.42 μm corresponding to base material. This initial grain size, along with the temperature, strain-rate and strain values predicted from the analytical models (from eq. 10), yields the final grain size distribution in the weld zone using the following equation suitable for continuous dynamic recrystallization

$$D_{CDRX} = 55\varepsilon^{-0.145}\dot{\varepsilon}^{-0.282}D_i^{-0.104}\exp\left(-\frac{Q}{RT}\right) \quad (11)$$

where the material constant terms are evaluated such that the error between calculated and experimental value is minimized. The constants in the equation were obtained by following an inverse approach using an optimization algorithm. The distribution of velocity and strain rate was evaluated at the same discretized point of finite element baser thermal model used to estimate temperature distribution. However, the effective points are considered at which point the experimental data are available. The values of activation energy (Q) and gas constant (R) assumed are 140 kJ/mole and 8.314 J/kg K, respectively. **Figure 5** shows the final prediction of grain size from analytical model. It shows relatively better agreement with experimental data at welding condition at 815 rpm and 63 mm/min welding speed.

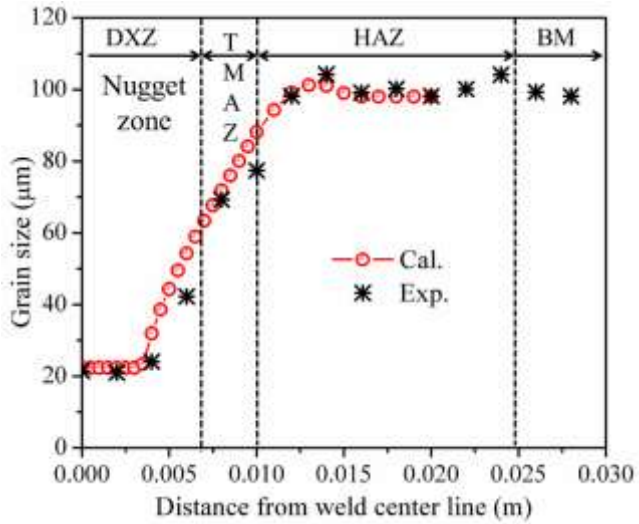

Figure 5: Calculated and experimentally measured grain size at different zone of friction stir welded sample at welding condition of 815 rpm and 63 mm/min welding speed.

Figure 6 shows the prediction of grain size distribution along a fixed line by incorporating the kinetics of CDRX (using eq. 11) as a function of strain, strain rate and temperature for fixed initial grain size. The maximum strain occurs close to the tool pin surface and therefore significant refinement in the grain size occurs in the nugget zone. It is indicated that the strain rate increases with increase in velocity field. The grain refinement decreases as move away from tool axis due to the decrease in effect of temperature and strain rate [8]. It's also observed that with increase in welding speed from 63 to 98 mm/min, the average grain size in the nugget has decreased considerably because of lesser heat input. As it is known, an increase in temperature leads to an increase in grain size (815 rpm and 63 mm/min welding speed) and, on the contrary, an increase in strain rate leads to a decrease in grain size (815 rpm and 98 mm/min welding speed) [329].

During FSW process, the material experiences severe plastic deformation and thermal exposure, this normally leads to formation of fine, recrystallized grain structure. The grain size of the nugget zone is measured from optical image that are depicted in **Fig. 7** for different welding conditions of Table 1. The average grain size for base materials is ~ 100 μm. After processing, the grain size in nugget zone at four different conditions varies between 20 μm to 23 μm. The increase in degree of deformation during FSW results in the reduction of grain size according to the general mechanism of recrystallization. The combination of lower temperature and shorter excursion time at the bottom of nugget effectively retards the grain growth and results in smaller recrystallized grains [286]. It is observed that lower rotational speed resulted in lower peak temperature and consequently the reduction in grain size due to higher plastic deformation and strain rate at low temperature [287-288]. At the circumference of the pin, the material flow is shown to be governed by the simple shear deformation induced by the rotating pin, which led to the formation of a fine equiaxed grains.

The grain size during CDRX strongly dependent on material parameters as a function of mainly strain rate and temperature. **Figure 8** illustrates the comparison between experimental and calculated grain size in the nugget zone corresponding to the welding condition of **Table 1**. The calculated grain size in the nugget zone ranges ~ 17 - 21 μm. It is obvious that the grain size of the stirred zone is reduced by increasing the traverse speed. The maximum effect of dynamic recrystallization and the minimum annealing effect on the welding heat input at higher traverse speed are responsible for fine refinement of grains. On other hand, an increase in the peak temperature with increase in rotation speed leads to generation of coarser recrystallized grains. Overall, the percentage error of grain size between calculated and experimental result is ~ 6 - 16 that is acceptable prediction for the present model. Although the above constitutive equation of grain size is validated for the present material, the analytical model for the estimation of strain rate will be able to work quite reasonably with different work piece materials. It requires an optimal design of process parameters for a target microstructure of FSW process.

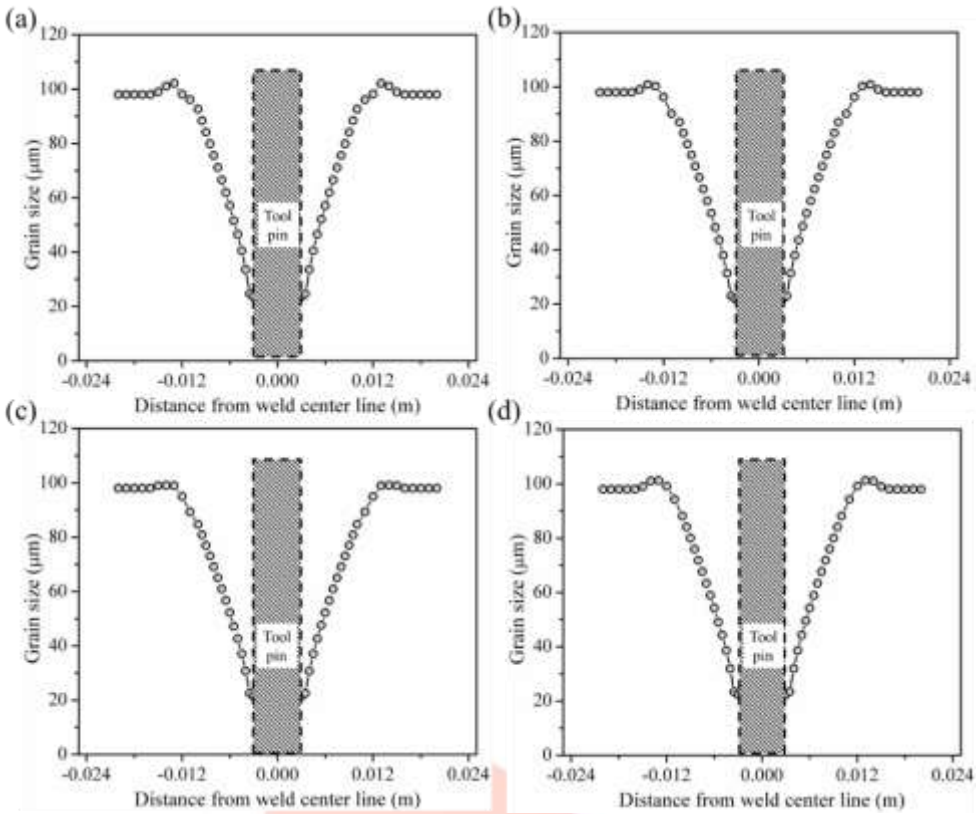

Figure 6: Estimation of grain size at the cross section 1 mm below top surface corresponding to welding condition of (a) Exp. No. 1, (b) Exp. No. 2, (c) Exp. No. 3, and (d) Exp. No. 4 of Table 1.

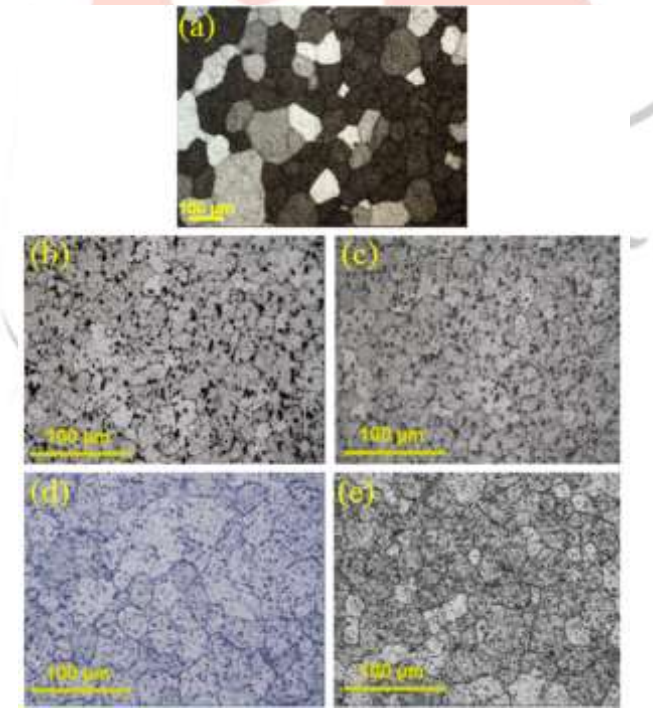

Figure 7: Microstructure of nugget zone: (a) base material; welding condition of (b) Exp. No. 1, (c) Exp. No. 2, (d) Exp. No. 3, and (e) Exp. No. 4 of Table 1.

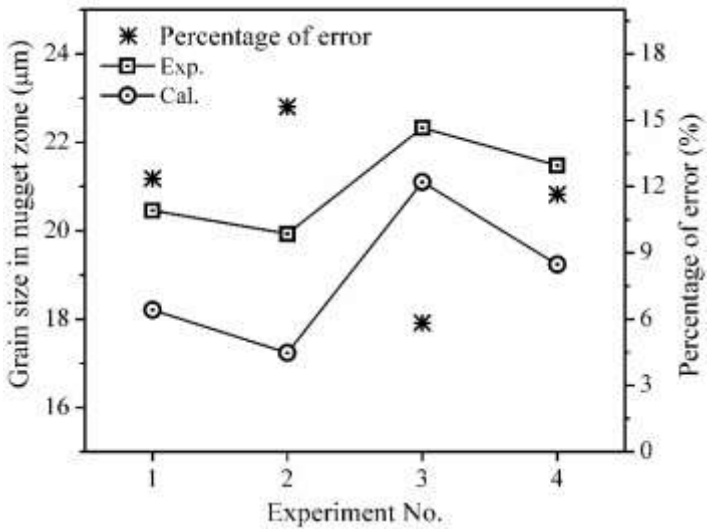

Figure 8: Experimental and estimated grain size in nugget zone with percentage of error.

Although a working model of CDRX is developed, the present work has several limitations that are the scope of work in near future. The model does not predict the recrystallization behaviour at the tool pin zone. There is need of experimental evidence for the existence of CDRX mechanism. An extensive experiment is required in the following welding conditions for the specified material. Normally transmission electron microscope (TEM) analysis is required to identify the existence of dislocations in the sample. The physical basis of the CDRX model may start from the one parameter model i.e. dislocation density based that evolves with respect to the condition of temperature, strain and strain rate. Since the domain of friction stir welded sample is subjected to variable temperature, strain and strain rate condition, a multi-scale model for the prediction of grain size distribution is a challenging task.

V. CONCLUSIONS

Recrystallization in heavily deformed material like FSW process is mainly governed by the condition of strain rate and temperature. Analytical model for the estimation of velocity field and corresponding effective strain rate and strain in the friction stir welded zone are developed. Using the condition of strain, strain rate and temperature, a constitutive model for continuous dynamic recrystallization is proposed. The constants are evaluated by an inverse approach using known experimental data. The model results are well agreed with experimental data. The following conclusions are derived from the present work.

- In friction stir welding of pure aluminum alloy, CRDX mechanism mainly prevails as observed form experiments. The temperature and strain rate conditions are main driving parameters for the recrystallization mechanism.
- Effective strain can be estimated from the velocity field in the domain of interest.
- The maximum strain rate adjacent to tool pin is achieved as 6 s^{-1} at the present welding condition.
- Very fine refinement of grains i.e. from 100 μm to 20 μm is achieved in the present set of experimental conditions.

REFERENCES

[1] A. Askari, S. Silling, B. London and M. Mahoney, "Friction Stir Welding and Processing," TMS, Warrendale, PA, pp. 43–50, 2001.
[2] K. V. Jata and S. L. Semiatin, "Continuous dynamic recrystallization during friction stir welding of high strength aluminum alloys," Scripta Mater., vol. 43, pp. 743–749, 2000.
[3] I. Charita and R. S. Mishra, "Abnormal grain growth in friction stir processed alloys," Scripta Mater., vol. 58, pp. 367–371, 2008.
[4] L. Liu, H. Nakayama, S. Fukumoto, A. Yamamoto and H. Tsubakino, "Microscopic observations of friction stir welded 6061 aluminum alloy," Mater. Trans., Vol. 45 (2), pp. 288 – 291, 2004
[5] K. S. Arora, S. Pandey, M. Schaper and R. Kumar, "Microstructure evolution during friction stir welding of aluminum alloy AA2219," J. Mater. Sci. and Tech., vol. 26(8), pp. 747-753, 2010.
[6] T. R. McNelley, S. Swaminathan and J. Q. Su, "Recrystallization mechanisms during friction stir welding/processing of aluminum alloys," Scripta Mater., vol. 58, pp. 349–354, 2008.
[7] P. Bernard, S. Bag, K. Huang and R. Logé, "A two-site mean field model of discontinuous dynamic recrystallization," Mater. Sci. and Eng. A, vol. 528(24), pp. 7357 - 7367, 2011.
[8] L. E. Murr, G. Liu, J. C. McClure, "Dynamic recrystallization in friction-stir welding of aluminium alloy 1100," J. Mater. Sci. Lett., vol. 16, pp. 1801-1803, 1997.
[9] F. J. Humphreys and M. Hatherly, Recrystallization and Related Annealing Phenomena, Pergamon Press, New York (1995).
[10] M. T. Lyttle and J. A. Wert, Advances in Hot Deformation Textures and Microstructures, ed. J. J. Jonas, T. R. Bieler, and K. J. Bowman, 1994, pp. 373–383, TMS, Warrendale, PA.

[11] B. M. Darras and M. K. Khraisheh, "Analytical modelling of strain rate distribution during friction stir processing," J. Mater. Eng. and Perform., vol. 17, pp. 168–177, 2008.
[12] S. Saluja, R. G. Narayanan and S. Das, "Cellular automata finite element (CAFE) model to predict the forming of friction stir welded blanks," Comp. Mater. Sci., vol. 58, pp. 87–100, 2012.
[13] Z. Zhang and J. T. Chen, "Computational investigations on reliable finite element-based thermo mechanical coupled simulations of friction stir welding," J. Adv. Manuf. Tech., vol. 60, pp. 959–975, 2012.
[14] G. Buffa, L. Fratini and R Shivpuri, "CDRX modelling in friction stir welding of AA7075-T6 aluminum alloy: analytical approaches," J. Mater. Proc. Tech., vol. 191, pg. 356–359, 2007.
[15] G. Buffa, J. Hua, R. Shivpuri and L. Fratini, "Design of the friction stir welding tool using the continuum based FEM model," Mater. Sci. and Eng. A, vol. 419, pp. 381–388, 2006.